



Plasma-assisted Modulation of Morphology and Composition in Tin Oxide Nanostructures for Sensing Applications



electrochromic devices, Solid state ionics 165, 181 (2003).

- [19] Amal Al-Kahlout ; Sabine Heusing ; Michel A. Aegerter, Electrochromism of NiO-TiO₂ sol gel layers, Journal of sol-gel Science and Technology, 39 (2), 195 (2006).
- [20] K.-S. Choi, S. Heusing, M.A. Aegerter, UV-gehärtete Sol-Gel-Ceroxid-Titanoxid-Schichten als Gegenelektrode für elektrochrome Fenster, Referate der Vorträge der 79. Glastechnischen Gesellschaft (DGG) 23. -25. Mai 2005, Würzburg.
- [21] www.ise.fhg.de
- [22] www.saint-gobain.com
- [23] www.refr-spd.com

Sanjay Mathur*, **Rajesh Ganesan**, **Thomas Ruegamer**, **Hao Shen**, **Sven Barth**

Detecting small quantities of gases and chemicals is becoming increasingly important for consumer, health and security applications such as monitoring the ecological constituents and to control the concentration of toxic and hazardous gases.[1] Nanostructures are especially attractive for detector and quantifier applications, particularly due to their high surface-to-volume ratio and higher sensitivity towards surface reactions, which results in charge penetration layers being comparable to nanostructure dimensions.[2] Tin oxide (SnO₂) represents the class of IV-VI com-

pound semiconductors with a wide band gap (3.6-4.0 eV) at room temperature and intrinsic n-type electrical conductivity.[3] Given their low electrical resistivity (10⁻²-10⁻⁴ Ωcm), high chemical resistance, thermal stability and mechanical strength,[4] SnO₂ nanostructures offer promising potential for improved chemical sensing behaviour due to its redox switching between different states, which facilitates a reversible transformation of the surface composition from Sn⁴⁺ cations on the surface into a reduced surface with Sn²⁺ cations depending on the oxygen chemical potential of the system.[5]

Tin oxide nanostructures have been synthesized by a number of methods such as chemical vapor transport at high temperatures,[6] thermal evaporation of tin oxide powders[7] and plasma enhanced chemical vapor deposition.[8] Although a large body of data is available on the synthesis of tin oxide nanostructures (particles, films, nanowires and nanobelts) in pure and doped compositions, synthetic pathways for their controlled growth and modification remains an overarching task. We have recently reported a molecule-based chemical vapor deposition (CVD) process for the synthesis of tin oxide and other semiconductor nanowires.[9-11]

The pre-formed Sn-O units in the precursor molecule $[\text{Sn}(\text{O}^t\text{Bu})_4]$ and the facile and clear stripping of organic ligands resulted in single crystalline SnO_2 nanowires at relatively low temperatures. [9] Herein we describe the controlled growth of single crystal tin oxide platelets followed by modulation of their morphology and composition induced by argon and oxygen plasma.

Semiconductor oxide nanostructures with ideal stoichiometric balance (electro-neutrality) are poor transducers for chemical sensing due to low signal-to-noise ratio, making excessive signal amplifications and/or high operating temperatures mandatory for optimal sensing performance. Since electrical properties of tin oxide depend on oxygen vacancies, mobility and concentration of charge carriers and surface states, an effective lowering of operation temperature and enhanced gas sensing ability can be obtained by modifying surface and chemical composition of stoichiometric nanostructures, for instance, through incorporation of metallic impurities in the oxide semiconductor. For example, an effective band bending effect can be achieved by increasing the concentration of donor atoms or defects in the material. We have exposed CVD grown tin oxide

nanoplates to a sputter-redeposition process in low power Ar/O_2 plasma, in order to modulate the defect concentration and the Sn:O stoichiometry followed by investigations on the chemical sensing properties of as-deposited and plasma treated samples.

Growth of tin oxide nanoplates: Crystal structure, composition and morphology

Tin oxide nanoplatelets were deposited by CVD of $[\text{Sn}(\text{O}^t\text{Bu})_4]$ in the temperature range $700\text{--}725\text{ }^\circ\text{C}$. Post-deposition modification of tin oxide nanostructures have been carried out by treating the samples (3 min) in r.f. plasma, as a versatile nano-modification and fabrication tool, containing reactive oxygen gas and argon carrier gas in 3:1 ratio. To study the influence of plasma treatment over the physical and chemical properties of the CVD grown tin oxide nanostructures (S1), samples were treated with the plasma powers of 25 (S2), 40 (S3), 55 (S4) and 125 (S5) W.

XRD patterns (figure 1) of as-deposited and plasma treated SnO_2 nanoplates showed a Cassiterite tetragonal rutile structure. No other crystalline impurities were detected in the samples. The intensity of the peaks corresponding to the SnO_2 phase was found to gradually diminish upon

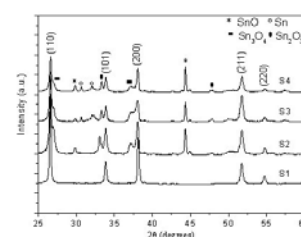


Fig. 1: XRD patterns of as-deposited (S1) and SnO_2 nanoplates treated with plasma powers 25 W (S2), 40 W (S3) and 55 W (S4), for 3 minutes.



plasma-treatment with increasing plasma power, which was accompanied by incipient crystallization of tin sub-oxides. Samples treated at 25 W plasma power (S2) revealed X-ray diffraction peaks corresponding to mix- and sub-valent tin oxide species (Sn_2O_3 , Sn_3O_4 and SnO) possibly formed by the etching of lattice oxygen atoms from the SnO_2 deposits. With further increase in plasma power (40 W), intensity of the peaks attributed to Sn_3O_4 and Sn_2O_3 were decreased apparently due to progressive reduction reactions, which was supported by the observation of metallic tin phase. Apparently, the enhanced etching of oxygen by high momentum particles impinging on the surface is responsible for the observed reduction of tin oxide.[8] It was also noted that the content of metallic Sn was proportional to the increase in applied plasma power. Treatment of tin oxide with pure Ar plasma produced samples with high tin content and conductance, which were not suitable for sensing applications.

The SEM analysis of S1 (figure 2) showed uniform SnO_2 nanoplates with the thickness of 30-40 nm, which were transformed to elongated granular structures by the ion bombardment at 25 W. The inhomogeneous morphological change suggested

a selective and preferential etching of certain facets in the nanoplates. Samples treated at higher plasma energy showed the formation of nanoglobular particles (samples S3 and S4), indicating advanced etching phenomenon and/or sputter-redeposition process. Given the reduced pressure in the plasma chamber (~ 4 Pa), the mean free path of the etched species was rather short which can lead to redeposition and rearrangement of etched tin and oxygen species on the surface of tin oxide platelets. At much higher plasma power (125 W), a large number of pores were found in the surface of the sample S5, exhibiting a predominant etching effect with suppressed redeposition.

XPS characterization of the samples S1, S3 and S5 (figure 3) confirmed the inherent changes observed in XRD, in the tin oxide CVD samples after exposure to r.f. plasma. As-deposited SnO_2 sample exhibited the characteristic double peak for the Sn 3d orbital with the main peak (Sn $3d_{5/2}$) at binding energy 486.6 eV (FWHM 1.4). Upon plasma treatment at 40 W, the appearance of an additional peak at lower binding energy (484.7 eV) was observed, which corresponds to the metallic tin phase.[12] The peak surface area analysis of the metallic phase revealed

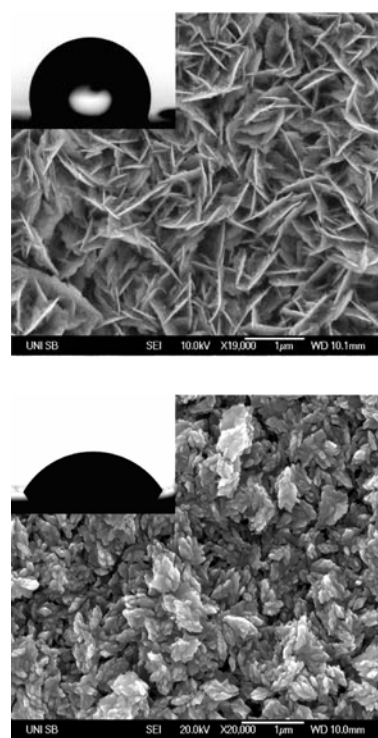


Fig. 2: SEM micrographs of (a) as deposited and (b) plasma-treated SnO_2 nanoplates along with their corresponding surface wetting behaviors.

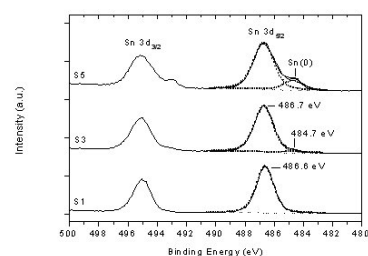


Fig. 3: XPS analysis of as-deposited and plasma-treated SnO_2 nanoplates.

approximately 3.0 at.% Sn(0) in the sample. XPS investigation of the sample S5, evidently showed that increased plasma energy (125 W) produced higher amount of metallic tin (up to 15.6 at.%), in accordance to the higher degree of chemical transformation.

Wetting behaviour and contact angle measurements

Interfering effects of water vapor in the detection of gaseous species on metal oxide surfaces is a well-known limitation (cross-sensitivity). Enhancement of gas sensing response in the presence of water vapor is commonly accepted although the corresponding mechanisms are complex and difficult to model. Since plasma treatment of SnO₂ surface can influence the degree of chemisorbed and rooted –OH groups (groups including lattice oxygen), the wetting properties of samples S1-S5 were investigated. Contact angle of water droplets on as-deposited and plasma treated nanoplates (Inset, figure 2) revealed a hydrophobic nature for as-deposited samples, with a contact angle of 108°. No notable changes were observed in the water repellent nature of sample S2 (contact angle 104°) treated at low plasma power (25 W). Samples treated at higher plasma po-

wers (S3 and S4) showed an increase in wetting behaviour with a decrease in the contact angles of 86° and 56°, respectively. The determination of contact angle on samples treated with 125 W was not possible and extreme hydrophilicity of the surface, evident in immediate film formation was observed.

Sensing characteristics

For chemical sensing experiments, 100 ppm ethanol in synthetic air was fed into the chamber with 15 sccm flow rate. The sensitivity of the SnO₂ samples was calculated as the ratio of its base resistance (R_{air}) to the shift due to ethanol exposure (R_{eth}).

Temperature dependent sensitivity of the samples treated at different plasma power conditions were measured by exposing the samples to air/ethanol/air cycles, in the temperature range 220 – 250 °C (figure 4). At 250 °C, the sensitivity towards ethanol molecules in samples S1, S2 and S3 was found to be 1.6, 2.1 and 5.9, respectively indicating a substantial augmentation of the gas sensing ability of SnO₂ deposits upon plasma treatment. Further increase in plasma power resulted in enhanced reduction of tin oxide as confirmed by higher metallic content (cf.

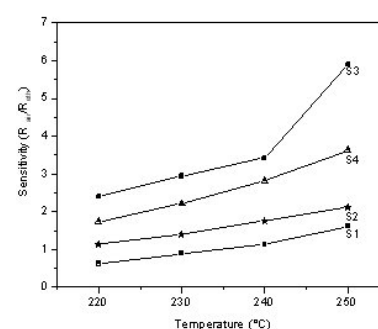


Fig. 4: Dependence of electrical response of tin oxide samples against operation temperature.



XRD), which reduced the sensitivity of the sample S4 to 3.6. In general, plasma treatment showed a positive effect on the gas sensing behaviour of as-deposited tin oxide deposits, which allowed to achieve substantial sensitivity of the samples even at lower operating temperature. However an increasing metallic character alters the conduction behaviour suppressing the semiconductor properties, detrimental for the transduction mechanism.

At room temperature, S3 (24.2 k Ω) showed lower resistance in comparison to S1 (44.1 k Ω), which can possibly be attributed to increased surface charge carriers in the oxygen deficient layers created through interaction of energetic species with surficial $-\text{Sn}-\text{O}-$ units. The sensing response cycles (figur 5) of S3, at 250 $^{\circ}\text{C}$ showed the base resistance of S3 was found to be higher than that of S1 apparently due to oxygen chemisorption at the newly generated active sites, which trap the electrons on the surface. Effective oxygen chemisorption, was favoured in non-stoichiometric S3 (cf. XRD and XPS), because neutral oxygen molecules adsorb in a more facile manner on plasma induced lattice oxygen vacancies and consequently, show better adsorption behaviour

over stoichiometric surfaces (S1). On exposure to ethanol gas at 250 $^{\circ}\text{C}$, the sheath resistance of S3 (-29 k Ω) was lower than that found in S1 (-67 k Ω) possibly due to redox reaction induced shift in the Fermi energy on the surface.[5] This also indicated the presence of partially reduced tin oxide species in S3, supporting higher chemisorption and therefore increased the molecular interactions between the reducing analyte and the surface, when compared to S1. As the chemisorbed oxygen atom does not attract the electrons so strongly as lattice atoms do, the resulted filled energy level is bent above the valence band. Since the segregated Sn atoms are expected to be less electropositive when compared to lattice bound Sn atoms, their energy levels are lower than the conduction band levels in stoichiometric tin oxide, as schematically described in figure 6.

As a result, new donor levels, created by plasma induced reduction, act as a source of additional charge carriers, which can be promoted to the surface with lower threshold energies, thus facilitating an effective redox reaction at lower temperature.

Plasma treatment at elevated power (55 W) apparently etched larger number of bridging oxygen atoms leading to pronounced SnO_2 reduc-

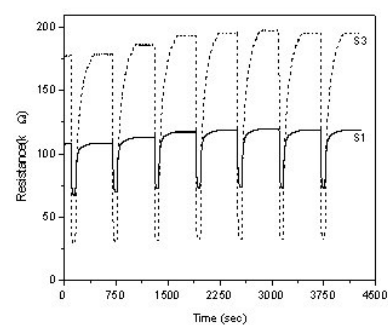


Fig. 5: Sensing response of S1 and S3 for ethanol at 250 $^{\circ}\text{C}$.

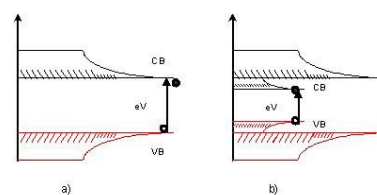


Fig. 6: Surface energy level model for SnO_2 suggesting the work function: (a) before and (b) after plasma treatment.

tion with formation of in-plane oxygen vacancies, which reduced the semiconductor properties and thus the sensitivity of the samples. The gradual chemical transformation model (figure 7), in as-deposited sample is evidenced by the emergence of Sn(0) peak as shown in the XRD and XPS data.

The response and recovery times were defined as the time needed for the resistance of the sensors to reach its final equilibrium value ($\pm 10\%$) for given reaction conditions (figure 8). Response time was nearly identical for all samples within the range of 10 seconds. Recovery time for S2 and S3 increased proportionally with higher plasma power used for surface modification whereas abrupt increase in recovery time for S4 suggested that removal (desorption) of chemisorbed oxygen in oxygen-deficient samples is energetically less favoured thereby demanding a longer time period to reach the equilibrium condition.

In summary, the plasma-chemical transformation of metal oxide nanostructures is a versatile strategy to modify the morphology, composition and functional behaviour of advanced ceramics with wide-reaching technological implication in the field of sensors and transparent conducting oxides.

References

- [1] M. I. Baraton, L. Mehari, J. Nanoparticle Res. 2004, 6, 107.
- [2] A. Kolmakov, M. Moskovits, Ann. Rev. Mat. Sci. 2004, 34, 151.
- [3] Y. J. Lin, C. J. Wu, Surf. and Coat. Tech. 1996, 88, 239.
- [4] Z. L. Wang in Nanowires and Nanobelts, Vol. 2 (Eds: Z. L. Wang), Springer, Berlin 2006, Ch. 1.
- [5] M. Batzill, U. Diebold, Prog. in Surf. Sci. 2005, 79, 47.
- [6] Z. R. Dai, J. L. Gole, J. D. Stout, Z. L. Wang, J. Phys. Chem. B 2002, 106, 1274.
- [7] E. Comini, G. Fagila, G. Sberveglieri, Appl. Phys. Lett. 2002, 81, 1869.
- [8] H. Huang, O. K. Tan, Y. C. Lee, M. S. Tse, J. Guo, T. White, Nanotech. 2006, 17, 243.
- [9] S. Mathur, S. Barth, H. Shen, J. C. Pyun, U. Werner, Small, 2005, 1, 713.
- [10] S. Mathur, H. Shen, V. Sivakov, U. Werner, Chem. Mater. 2004, 16, 2449.
- [11] S. Mathur, T. Ruegamer, N. Donia, H. Shen, J. Nanosci. Nanotech. 2007 (accepted).
- [12] M. Veith, N. Lecerf and S. Mathur, H. Shen, S. Huefner, Chem. Mater. 1999, 11, 3013-39 (1973)

Acknowledgement: Authors thank the Saarland state and central government for providing financial assistance. The German Science Foundation (DFG) is gratefully acknowledged for supporting our research (priority program SFB-277 "Grenzflächenbestimmte Materialien")

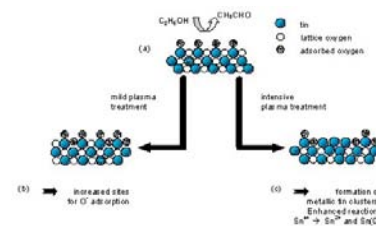


Fig. 7: Schematic representation of Sn:O stoichiometry in as-deposited and plasma-treated samples.

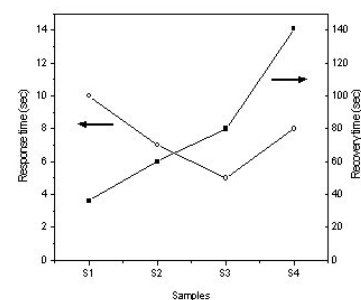


Fig. 8: Response and recovery times of SnO₂ nanoplates for ethanol sensing.